

Synthesis, Crystal Structures, and Magnetic Properties of Dinuclear and Hexanuclear Copper(II) Complexes with Cyclam-Based Macrocyclic Ligands Having Four Schiff-Base Pendant Arms

Shusaku Wada, Koki Saka, Daisuke Yoshioka, and Masahiro Mikuriya*

Department of Chemistry, School of Science and Technology, Kwansei Gakuin University, 2-1 Gakuen, Sanda 669-1337

Received October 28, 2009; E-mail: junpei@kwansei.ac.jp

Reaction of a series of dodecadentate ligands (H_4L), 1,4,8,11-tetrakis(salicylideneaminoethyl)-1,4,8,11-tetraazacyclotetradecane and its substituted derivatives, with copper(II) salts afforded dinuclear copper(II) complexes, [Cu_2L], which were characterized by IR and UV–vis–NIR spectroscopy, and temperature dependence of magnetic susceptibilities (4.5–300 K). Single-crystal X-ray crystallography of these complexes revealed that each copper(II) ion is bound by the chelating of the two Schiff-base pendant arms outside the central tetraazacyclotetradecane ring forming a distorted square plane with an intramolecular Cu–Cu distance of 8.692(2)–8.949(2) Å. In accordance with the crystal structures, the magnetic interaction between the two copper(II) atoms is very weak. In the case of 1,4,8,11-tetrakis(3-methoxysalicylideneaminoethyl)-1,4,8,11-tetraazacyclotetradecane (H_4tmsaec), a hexanuclear complex with a crystallographic inversion center, [$Cu_6(O_2CCH_3)_8$(tmsaec)], was isolated. In the asymmetric unit, one copper atom is bonded to one pendant arm and two copper atoms are bound to another pendant arm with the methoxy group of the Schiff-base moiety with the Cu–Cu distance of 3.096(1) Å, giving a novel system containing monodentate, bidentate, and bridging acetate ions in the same molecule. Magnetic susceptibility data shows that a weak antiferromagnetic interaction is operating between the closest two copper atoms.

Chemistry of macrocyclic polyamine ligands with pendant arms has attracted much interest over the past two decades, because of their specific structures and chemical properties, high ability as molecular recognition ability of anions or cations, and applications from radiopharmaceutical chemistry to waste-water treatment.[1,2] Habitually, these macrocyclic polyamine ligands bind one metal ion at the center of the macrocyclic cavity forming 1:1 molar ratio complexes. Among macrocyclic ligands with pendant arms, an octadentate ligand, 1,4,8,11-tetrakis(2-aminoethyl)-1,4,8,11-tetraazacyclotetradecane (abbreviated as taec), is unique, forming exclusively dinuclear metal species without any metal ion in the macrocyclic ring.[3] This could be ascribed to the high coordination ability of the pendant amino groups compared with the donation of the tertiary amine nitrogen atoms of the 1,4,8,11-tetraazacyclotetradecane (cyclam) moiety. A related tetratosylated taec derivative, 1,4,8,11-tetrakis(2-*p*-toluenesulfonamidoethyl)-1,4,8,11-tetraazacyclotetradecane (H_4tstaec), which was expected to bind one metal ion in the macrocyclic ring because of the poor donating property of the tosylated amino groups, also binds two metal ions outside the macrocyclic ring, giving a dinuclear metal species.[4] Recently, we designed new cyclam-based Schiff-base ligands by functionalization of 1,4,8,11-tetraazacyclotetradecane with four salicylideneaminoethyl groups as pendant arms (Chart 1) in order to obtain manganese species which were difficult to get by the taec and H_4tstaec ligands.[5] These potential dodecadentate ligands, 1,4,8,11-tetrakis(salicylideneaminoethyl)-cyclam (H_4tsaec) and its substituent derivatives, do not bind one metal ion within the macrocyclic ring, but form dinuclear manganese(III) complexes by reaction with Mn^{II} ion. The two Mn^{III} ions are coordinated by two pairs of the pendant Schiff-base groups outside the macrocyclic ring moiety, resulting in a long Mn···Mn separation of 9.676(4)–10.096(2) Å. Formation of manganese(III) species may be understandable by the presence of tetradentate N_2O_2 donor atoms of the Schiff-base groups in these ligands, because many manganese(III) complexes can be prepared from reactions of manganese(II) salts and Schiff-base ligands containing N and O donor atoms.[6] In these complexes, the manganese(III) atoms are invoked by a Jahn–Teller distortion. The present ligand systems are expected to be used for other metal ions such as copper(II), because copper(II) is also invoked by a Jahn–Teller distortion in octahedral geometry and prefers five- or four-coordinate geometries. In this context, we explored copper(II) complexes with these dodecadentate Schiff-base ligands and obtained dinuclear copper(II) complexes. We also synthesized disubstituted derivatives of the Schiff-base ligands (Chart 1), tetrakis(3,5-dibromosalicylideneaminoethyl)cyclam (H_4tdbsaec) and tetrakis(3,5-dichlorosalicylideneaminoethyl)cyclam (H_4tdcsaec), and prepared their dinuclear copper(II) complexes. Surprisingly, using a similar synthetic procedure, we isolated a hexanuclear copper(II) complex in the case of 1,4,8,11-tetrakis(3-methoxysalicylideneaminoethyl)-1,4,8,11-tetraazacyclotetradecane (H_4tmsaec). We report here, the synthesis and structural and magnetic characterization of these copper(II) complexes with the cyclam-based dodecadentate Schiff-base ligands.

Experimental

Synthesis. Unless otherwise specified, all reagents were

Published on the web March 18, 2010; doi:10.1246/bcsj.20090284

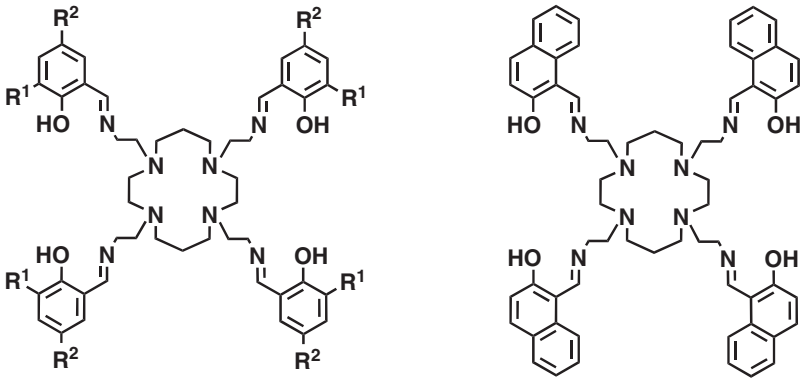

Chart 1. (a) H_4tsaec (R^1, $R^2 = H$), H_4tbsaec ($R^1 = H$, $R^2 = Br$), H_4tcsaec ($R^1 = H$, $R^2 = Cl$), H_4tdbsaec (R^1, $R^2 = Br$), H_4tdcsaec (R^1, $R^2 = Cl$), and H_4tmsaec ($R^1 = OCH_3$, $R^2 = H$). (b) H_4tnaec.

purchased commercially and used without further purification.

Macrocyclic Ligands. The dodecadentate ligands, tetrakis-(salicylideneaminoethyl)cyclam analogs, H_4tbsaec, H_4tcsaec, and H_4tnaec, were synthesized by the condensation reaction between taec and the corresponding salicylaldehyde derivatives according to the previously reported procedure.[5]

Tetrakis(3,5-dibromosalicylideneaminoethyl)cyclam (H_4tdbsaec). To a stirred solution of taec (107 mg, 0.24 mmol) in methanol (10 mL) was added a methanol solution (5 mL) of 3,5-dibromosalicylaldehyde (271 mg, 0.97 mmol). The resulting yellow precipitate was filtered off and washed with methanol. Yield: 292 mg (86%). Anal. Found: C, 39.08; H, 3.53; N, 7.94%. Calcd for $C_{46}H_{52}Br_8N_8O_4$: C, 38.90; H, 3.69; N, 7.89%. IR(KBr): ν(ArH) 3056, $\nu_{as}(CH_2)$ 2947, $\nu_s(CH_2)$ 2795, ν(C=N) 1646 cm^{-1}. UV–vis: λ_{max} ($\varepsilon/M^{-1}\,cm^{-1}$, measured in $CHCl_3$) 286 (16100), 336 (12000), 432 nm (11600). Diffused reflectance spectrum: λ_{max} 228, 282, 342, 408, 445 nm.

Tetrakis(3,5-dichlorosalicylideneaminoethyl)cyclam (H_4tdcsaec). This ligand was obtained as yellow precipitate by the reaction of taec (80 mg, 0.22 mmol) and 3,5-dichlorosalicylaldehyde (165 mg, 0.86 mmol) in methanol using the same method as that of H_4tdbsaec. Yield: 153 mg (77%). Anal. Found: C, 52.08; H, 4.63; N, 10.53%. Calcd for $C_{46}H_{52}Cl_8N_8O_4$: C, 51.90; H, 4.92; N, 10.53%. IR(KBr): ν(ArH) 3050, $\nu_{as}(CH_2)$ 2960, $\nu_s(CH_2)$ 2808, ν(C=N) 1650 cm^{-1}. UV–vis: λ_{max} ($\varepsilon/M^{-1}\,cm^{-1}$, measured in $CHCl_3$) 283 (14400), 335 (12400), 432 nm (9170). Diffused reflectance spectrum: λ_{max} 227, 281, 341, 403, 443 nm.

[Cu_2(tsaec)]·0.5H_2O (1·0.5H_2O). Taec (30 mg, 0.08 mmol) was dissolved in methanol (4 mL) at room temperature. To this solution was added a methanol solution (2 mL) of salicylaldehyde (40 mg, 0.33 mmol), 6 mL of chloroform, and copper(II) acetylacetonate (42 mg, 0.16 mmol), and the mixture was stirred for 10 min, and then filtered. On to the resulting green solution was layered methanol (6 mL), and the mixture was then allowed to stand at room temperature to give green crystals. Yield: 46 mg (52%). Anal. Found: C, 60.17; H, 6.26; N, 12.00%. Calcd for $C_{46}H_{56}Cu_2N_8O_4$·0.5H_2O: C, 59.98; H, 6.24; N, 12.16%. IR(KBr): ν(ArH) 3052, $\nu_{as}(CH_2)$ 2941, $\nu_s(CH_2)$ 2797, ν(C=N) 1636 cm^{-1}. Diffuse reflectance spectrum: λ_{max} 227, 279, 304, 378, 470sh, 643, 845sh nm.

[Cu_2(tbsaec)]·H_2O (2·H_2O). H_4tbsaec (48 mg, 0.043 mmol) was dissolved in chloroform (30 mL). To this solution was added an acetonitrile solution (60 mL) of copper(II) acetate (16 mg, 0.088 mmol). The mixture was allowed to stand at room temperature to give green crystals. Yield: 42 mg (78%). Anal. Found: C, 44.08; H, 4.08; N, 9.27%. Calcd for $C_{46}H_{52}Br_4Cu_2N_8O_4$·$H_2O$: C, 44.35; H, 4.37; N, 8.99%. IR(KBr): $\nu_{as}(CH_2)$ 2920, $\nu_s(CH_2)$ 2795, ν(C=N) 1629 cm^{-1}. Diffuse reflectance spectrum: λ_{max} 306, 390, 660 nm.

[Cu_2(tdbsaec)]·$CHCl_3$ (3·$CHCl_3$). H_4tdbsaec (54 mg, 0.038 mmol) was dissolved in chloroform (45 mL). To this solution was added an acetonitrile solution (45 mL) of copper(II) acetate (15 mg, 0.083 mmol). The mixture was allowed to stand at room temperature to give green crystals. Yield: 44 mg (71%). Anal. Found: C, 34.00; H, 2.83; N, 6.75%. Calcd for $C_{46}H_{48}Br_8Cu_2N_8O_4$·$CHCl_3$: C, 33.95; H, 2.97; N, 6.74%. IR(KBr): ν(ArH) 3063, $\nu_{as}(CH_2)$ 2940, $\nu_s(CH_2)$ 2810, ν(C=N) 1632 cm^{-1}. Diffuse reflectance spectrum: λ_{max} 224, 298, 387, 470sh, 656, 790sh nm.

[Cu_2(tcsaec)]·0.5CH_3CN·H_2O (4·0.5CH_3CN·H_2O). H_4tcsaec (47 mg, 0.051 mmol) was dissolved in $CHCl_3$ (30 mL). To this solution was added an CH_3CN solution (60 mL) of copper(II) acetate (19 mg, 0.105 mmol). The mixture was allowed to stand at room temperature to give green crystals. Yield: 48 mg (86%). Anal. Found: C, 51.99; H, 4.83; N, 10.96%. Calcd for $C_{46}H_{52}Cl_4Cu_2N_8O_4$·0.5$CH_3CN$·$H_2O$: C, 51.87; H, 5.14; N, 10.94%. IR(KBr): ν(ArH) 3008, $\nu_{as}(CH_2)$ 2924, $\nu_s(CH_2)$ 2796, ν(C=N) 1629 cm^{-1}. Diffuse reflectance spectrum: λ_{max} 303, 388, 661 nm.

[Cu_2(tdcsaec)]·$CHCl_3$·3H_2O (5·$CHCl_3$·3H_2O). The complex was prepared in the same way as **3**·$CHCl_3$, except that H_4tdcsaec was used instead of H_4tdbsaec. Yield: 48 mg (70%). Anal. Found: C, 41.58; H, 3.90; N, 8.46%. Calcd for $C_{46}H_{48}Cl_8Cu_2N_8O_4$·$CHCl_3$·3$H_2O$: C, 41.48; H, 4.07; N, 8.23%. IR(KBr): ν(ArH) 3073, $\nu_{as}(CH_2)$ 2941, $\nu_s(CH_2)$ 2810, ν(C=N) 1633 cm^{-1}. Diffuse reflectance spectrum: λ_{max} 230, 295, 383, 642 nm.

[Cu_2(tnaec)]·2$CHCl_3$·H_2O (6·2$CHCl_3$·H_2O). H_4tnaec (45 mg, 0.045 mmol) was dissolved in $CHCl_3$ (30 mL). To this solution was added an CH_3CN solution (30 mL) of copper(II) acetate (17 mg, 0.094 mmol). The mixture was allowed to stand at room temperature to give green crystals. Yield: 47 mg (75%). Anal. Found: C, 56.08; H, 4.66; N, 8.48%. Calcd for $C_{62}H_{64}Cu_2N_8O_4$·2$CHCl_3$·H_2O: C, 56.15; H, 5.01; N, 8.19%. IR(KBr): ν(ArH) 3061, $\nu_{as}(CH_2)$ 2968, $\nu_s(CH_2)$ 2802, ν(C=N) 1619 cm^{-1}. Diffuse reflectance spectrum: λ_{max} 226, 315, 401, 647 nm.

[$Cu_6(O_2CCH_3)_8$(tmsaec)]·3H_2O (7·3H_2O). Taec (51 mg, 0.137 mmol) was dissolved in CH_3CN (20 mL) at 60 °C. To this solution was added 3-methoxysalicylaldehyde (83 mg, 0.55 mmol), copper(II) acetate (99 mg, 0.55 mmol), and the mixture was heated at 60 °C for 10 min, and then filtered. The resulting green solution

Table 1. Crystal Data and Data Collection Details

	$[Cu_2(tsaec)]\cdot 2CHCl_3$ (**1**·2$CHCl_3$)	$[Cu_2(tbsaec)]\cdot CHCl_3$ (**2**·$CHCl_3$)	$[Cu_2(tdbsaec)]\cdot 2/3CHCl_3\cdot 8/3H_2O$ (**3**·2/3$CHCl_3$·8/3H_2O)	$[Cu_2(tcsaec)]\cdot CHCl_3$ (**4**·$CHCl_3$)	$[Cu_2(tdcsaec)]\cdot 2/3CHCl_3\cdot 8/3H_2O$ (**5**·2/3$CHCl_3$·8/3H_2O)	$[Cu_2(tnaec)]\cdot 2CH_3CN$ (**6**·2CH_3CN)	$[Cu_6(O_2CCH_3)_8(tmsaec)]\cdot 2CH_3CN\cdot 11H_2O$ (**7**·2CH_3CN·11H_2O)
Formula	$C_{48}H_{58}Cl_6Cu_2N_8O_4$	$C_{47}H_{53}Br_4Cl_3Cu_2N_8O_4$	$C_{46.66}H_{54}Br_8Cl_2Cu_2N_8O_{6.66}$	$C_{47}H_{53}Cl_7Cu_2N_8O_4$	$C_{46.66}H_{54}Cl_{10}Cu_2N_8O_{6.66}$	$C_{66}H_{70}Cu_2N_{10}O_4$	$C_{70}H_{116}Cu_6N_{10}O_{35}$
FW	1150.80	1346.04	1670.91	1169.20	1315.23	1194.40	2038.97
Temperature/K	293	123	293	293	293	293	123
Crystal system	Triclinic	Triclinic	Trigonal	Triclinic	Trigonal	Monoclinic	Monoclinic
Space group	$P\bar{1}$	$P\bar{1}$	$R\bar{3}$	$P\bar{1}$	$R\bar{3}$	$P2_1/c$	$P2_1/n$
a/Å	10.772(13)	13.517(3)	27.058(15)	13.511(2)	26.756(5)	17.159(5)	13.059(3)
b/Å	13.900(16)	14.984(3)		15.020(3)		11.911(3)	23.657(5)
c/Å	18.73(2)	15.119(3)	21.463(17)	15.097(3)	21.191(5)	16.011(5)	14.440(3)
α/°	88.06(2)	64.041(4)		114.827(3)			
β/°	74.54(3)	65.343(3)		114.785(3)		115.440(5)	102.488(4)
γ/°	70.17(3)	89.644(4)		90.437(3)			
V/Å^3	2538(5)	2443.1(9)	13609(16)	2461.0(7)	13138(5)	2955.1(13)	4355.7(15)
Z	2	2	9	2	9	2	2
D_{calcd}/g cm^{-3}	1.51	1.83	1.84	1.58	1.50	1.34	1.56
D_m/g cm^{-3}	1.52	1.80	1.81	1.56	1.51	1.33	1.54
Crystal size/mm^3	0.45 × 0.43 × 0.18	0.42 × 0.23 × 0.10	0.18 × 0.12 × 0.08	0.47 × 0.43 × 0.38	0.27 × 0.25 × 0.10	0.43 × 0.38 × 0.30	0.35 × 0.13 × 0.08
μ(Mo Kα)/mm^{-1}	1.206	4.359	6.128	1.298	1.239	0.778	1.529
θ range/°	1.56–29.07	1.55–28.45	1.29–28.27	1.53–28.37	1.52–28.58	2.16–28.55	1.68–28.59
No. of reflections	16386	14967	28129	15118	27578	17858	26423
No. of unique reflections	11669	10650	7167	10775	6936	6843	10102
$R1$ [$I > 2\sigma(I)$], $wR2$ [all data][a)]	0.0525, 0.1265	0.0631, 0.2003	0.0564, 0.1856	0.0617, 0.2032	0.0792, 0.2607	0.0401, 0.0779	0.0879, 0.2297
Goodness-of-fit on F^2	0.738	1.086	0.798	0.990	0.860	0.821	1.013

a) $R1 = \Sigma||F_o| - |F_c||/\Sigma|F_o|$, $wR2 = [\Sigma w(F_o^2 - F_c^2)^2/\Sigma w(F_o^2)^2]^{1/2}$.

was allowed to stand at room temperature to give green crystals. Yield: 105 mg (43%). Anal. Found: C, 43.80; H, 5.41; N, 5.91%. Calcd for $C_{66}H_{88}Cu_6N_8O_{24}\cdot 3H_2O$: C, 43.73; H, 5.23; N, 6.18%. IR(KBr): ν(OH) 3423 br, $\nu_{as}(CH_2)$ 2966, $\nu_s(CH_2)$ 2839, ν(C=N) 1635, $\nu_{as}(CO_2)$ 1620, $\nu_{as}(CO_2)$ 1569, $\nu_{as}(CO_2)$ 1540sh, $\nu_s(CO_2)$ 1439, $\nu_s(CO_2)$ 1416, $\nu_s(CO_2)$ 1390sh cm^{-1}. UV–vis: λ_{max} ($\varepsilon/M^{-1}\,cm^{-1}$, measured in DMSO) 384 (15800), 670 nm (793). Diffuse reflectance spectrum: λ_{max} 239, 283, 381, 480sh, 696, 900sh nm.

Measurements. Elemental analyses of carbon, hydrogen, and nitrogen were conducted using a Thermo Finnigan FLASH EA 1112 series CHNO-S Analyzer. Infrared spectra were measured with a JASCO MFT-2000 FT-IR Spectrometer in the 4000–600 cm^{-1} region. The electronic spectra were measured with a Shimadzu UV–vis–NIR Recording Spectrophotometer Model UV-3100. The temperature dependence of the magnetic susceptibilities was measured with a Quantum Design MPMS-5S SQUID susceptometer operating at a magnetic field of 0.5 T over a temperature range of 4.5–300 K. The susceptibilities were corrected for the diamagnetism of constituent atoms using Pascal's constants.[7] The effective magnetic moments were calculated from the equation $\mu_{eff} = 2.828\sqrt{\chi_A T}$, where χ_A is the atomic magnetic susceptibility.

X-ray Crystal Structure Analyses. A preliminary examination was made and data were collected on a Bruker CCD X-ray diffractometer (SMART APEX) using graphite-monochromated Mo Kα radiation. Crystal data and details concerning data collection are given in Table 1. The structures were solved by direct methods, and refined by full-matrix least-squares methods. The hydrogen atoms except those bound to the water oxygen atoms were inserted at their calculated positions and fixed there. All of the calculations were carried out on a Pentium IV Windows 2000 computer utilizing the SHELXTL software package.[8] Crystallographic data have been deposited with Cambridge Crystallographic Data Centre: Deposit number CCDC-743870–743876. Copies of the data can be obtained free of charge via http://www.ccdc.cam.ac.uk/conts/retrieving.html (or from the Cambridge Crystallographic Data Centre, 12, Union Road, Cambridge, CB2 1EZ, U.K.; Fax: +44 1223 336033; e-mail: deposit@ccdc.cam.ac.uk).

Results and Discussion

Dinuclear Copper(II) Complexes with the Dodecadentate Ligands, [Cu_2(L)] (L = tsaec^{4-}, tbsaec^{4-}, tdbsaec^{4-}, tcsaec^{4-}, tdcsaec^{4-}, and tnaec^{4-}). The synthesis of the dinuclear copper(II) complexes was achieved by the reaction of the dodecadentate Schiff-base ligands (H_4L) and copper(II) salt in a 1:2 molar ratio in chloroform–acetonitrile solution in good yields. In the case of H_4tsaec, we used a template reaction in methanol to prepare the copper(II) complex because of the difficulty in isolating the Schiff-base ligand by the reaction of taec and salicylaldehyde. Elemental analyses confirmed a stoichiometry of [Cu_2(L)] with solvent molecules. Contrary to the case for the manganese(III) complexes,[5] the complexes are neutral without any counter anion such as acetate ion. The complexes show a strong IR band at around 1630 cm^{-1} attributable to ν(C=N) stretching vibration. This band is shifted to a lower frequency (ca. 10 cm^{-1}) compared with those of the Schiff-base ligands as expected from coordination of the imino-nitrogen to the copper atom. Single crystals suitable for X-ray diffraction study were obtained from a diffusion method

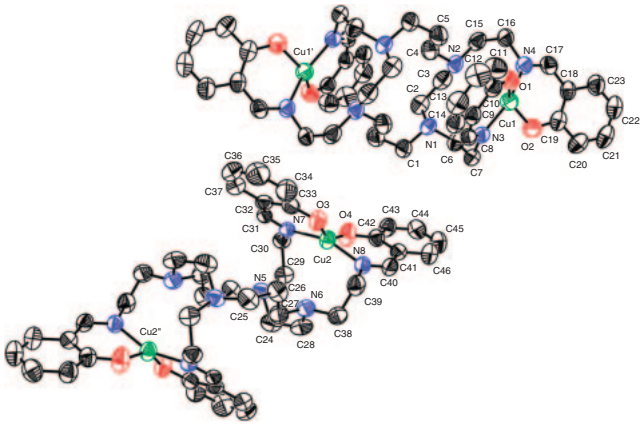

Figure 1. ORTEP drawing of the structure of [Cu_2(tsaec)]·2$CHCl_3$ (**1**·2$CHCl_3$) showing the 50% probability thermal ellipsoids and atom numbering scheme. Hydrogen atoms and solvent molecules are omitted for clarity.

similar to the condition for the synthesis of the copper(II) complexes. The crystal structures were determined by X-ray crystal structure analysis for [Cu_2(tsaec)]·2$CHCl_3$ (**1**·2$CHCl_3$), [Cu_2(tbsaec)]·$CHCl_3$ (**2**·$CHCl_3$), [Cu_2(tdbsaec)]·2/3$CHCl_3$·8/3H_2O (**3**·2/3$CHCl_3$·8/3H_2O), [Cu_2(tcsaec)]·$CHCl_3$ (**4**·$CHCl_3$), [Cu_2(tdcsaec)]·2/3$CHCl_3$·8/3H_2O (**5**·2/3$CHCl_3$·8/3H_2O), [Cu_2(tnaec)]·2CH_3CN (**6**·2CH_3CN). An ORTEP drawing of the crystal structure of **1**·2$CHCl_3$ is shown in Figure 1 together with the atomic numbering scheme. Selected bond distances and angles are listed in Table 2. There are two crystallographically independent dinuclear complexes in the crystal. Both of the complex molecules possess a crystallographic inversion center and are similar to each other. In each dinuclear molecule, two copper atoms are bound by two pairs of the Schiff-base pendant arms below and above the cyclam ring moiety of tsaec^{4-} ligand. The Cu···Cu distances within the dinuclear molecules are 8.833(8) [Cu1···Cu1′] and 8.756(9) Å [Cu2···Cu2″]. Each copper atom is coordinated by two imino-nitrogen atoms (N3 and N4 for Cu1, N7 and N8 for Cu2) and two phenolic-oxygen atoms (O1 and O2 for Cu1, O3 and O4 for Cu2) of the Schiff-base pendant arms in a square-planar arrangement. However, the planes defined by O1–N3–O2–N4 and O3–N7–O4–N8 deviate from the strict planar configuration within ±0.46 Å, and the Cu1 and Cu2 atoms are 0.13 and 0.10 Å below these mean planes, respectively. The Cu–O (1.863(3)–1.888(4) Å) and Cu–N distances (1.919(4)–1.937(4) Å) fall in the range of the values reported for square-planar copper(II) complexes of tetradentate N_2O_2 Schiff-base ligands.[9] The cyclam ring moiety of tsaec^{4-} adopts the trans-IV configuration[10] similar to the dinuclear manganese complexes with this type of dodecadentate Schiff-base ligands.[5] This configuration can be also found in the dinuclear palladium complex of tstaec^{4-} with bulky functional groups.[4] The closest intermolecular Cu···Cu distance is 7.367(9) Å of Cu1···Cu2 (x, $y+1$, z), being shorter than the intramolecular Cu···Cu distances. The crystal contains chloroform molecules which form closest contacts with the phenolic-oxygen atoms of the Schiff-base ligands [O1···C47 ($CHCl_3$) 3.133(6) Å and O3···C48 ($CHCl_3$) 3.110(6) Å].

Table 2. Selected Bond Distances/Å and Angles/° with Their Estimated Standard Deviations in Parentheses

$[Cu_2(tsaec)]\cdot 2CHCl_3$ (**1**$\cdot 2CHCl_3$)			
Cu1–O1	1.888(4)	Cu2–O3	1.875(4)
Cu1–O2	1.870(4)	Cu2–O4	1.863(3)
Cu1–N3	1.920(4)	Cu2–N7	1.937(4)
Cu1–N4	1.919(4)	Cu2–N8	1.935(3)
O1–Cu1–O2	143.7(1)	O3–Cu2–O4	145.8(1)
O1–Cu1–N3	94.7(2)	O3–Cu2–N7	94.6(1)
O1–Cu1–N4	92.3(1)	O3–Cu2–N8	93.3(1)
O2–Cu1–N3	92.4(1)	O4–Cu2–N7	90.9(1)
O2–Cu1–N4	92.6(1)	O4–Cu2–N8	93.1(2)
N3–Cu1–N4	160.5(1)	N7–Cu2–N8	159.6(1)
$[Cu_2(tbsaec)]\cdot CHCl_3$ (**2**$\cdot CHCl_3$)			
Cu1–O1	1.926(4)	Cu2–O3	1.923(5)
Cu1–O2	1.915(4)	Cu2–O4	1.956(5)
Cu1–N3	1.957(5)	Cu2–N7	1.959(5)
Cu1–N4	1.943(5)	Cu2–N8	1.975(6)
O1–Cu1–O2	145.2(2)	O3–Cu2–O4	156.7(2)
O1–Cu1–N3	93.9(2)	O3–Cu2–N7	93.4(2)
O1–Cu1–N4	93.9(2)	O3–Cu2–N8	90.2(2)
O2–Cu1–N3	90.4(2)	O4–Cu2–N7	91.5(2)
O2–Cu1–N4	92.0(2)	O4–Cu2–N8	89.1(2)
N3–Cu1–N4	162.5(2)	N7–Cu2–N8	169.3(2)
$[Cu_2(tdbsaec)]\cdot 2/3CHCl_3\cdot 8/3H_2O$ (**3**$\cdot 2/3CHCl_3\cdot 8/3H_2O$)			
Cu1–O1	1.899(6)	Cu1–N3	1.960(8)
Cu1–O2	1.925(6)	Cu1–N4	1.941(8)
O1–Cu1–O2	153.7(3)	O2–Cu1–N3	93.1(3)
O1–Cu1–N3	92.8(3)	O2–Cu1–N4	88.5(3)
O1–Cu1–N4	90.1(3)	N3–Cu1–N4	170.0(3)
$[Cu_2(tcsaec)]\cdot CHCl_3$ (**4**$\cdot CHCl_3$)			
Cu1–O1	1.906(3)	Cu2–O3	1.953(3)
Cu1–O2	1.924(3)	Cu2–O4	1.926(3)
Cu1–N3	1.951(3)	Cu2–N7	1.972(4)
Cu1–N4	1.957(3)	Cu2–N8	1.966(3)
O1–Cu1–O2	144.2(1)	O3–Cu2–O4	155.8(1)
O1–Cu1–N3	92.1(1)	O3–Cu2–N7	88.4(2)
O1–Cu1–N4	90.9(1)	O3–Cu2–N8	91.7(1)
O2–Cu1–N3	95.1(1)	O4–Cu2–N7	90.9(1)
O2–Cu1–N4	93.3(1)	O4–Cu2–N8	93.5(1)
N3–Cu1–N4	161.1(1)	N7–Cu2–N8	168.9(1)
$[Cu_2(tdcsaec)]\cdot 2/3CHCl_3\cdot 8/3H_2O$ (**5**$\cdot 2/3CHCl_3\cdot 8/3H_2O$)			
Cu1–O1	1.924(5)	Cu1–N3	1.940(6)
Cu1–O2	1.887(5)	Cu1–N4	1.964(6)
O1–Cu1–O2	153.4(2)	O2–Cu1–N3	91.9(2)
O1–Cu1–N3	87.8(2)	O2–Cu1–N4	92.5(2)
O1–Cu1–N4	92.6(2)	N3–Cu1–N4	169.3(3)
$[Cu_2(tnaec)]\cdot 2CH_3CN$ (**6**$\cdot 2CH_3CN$)			
Cu1–O1	1.905(2)	Cu1–N3	1.936(2)
Cu1–O2	1.920(2)	Cu1–N4	1.947(2)
O1–Cu1–O2	151.60(7)	O2–Cu1–N3	91.80(7)
O1–Cu1–N3	92.73(7)	O2–Cu1–N4	90.06(7)
O1–Cu1–N4	92.92(7)	N3–Cu1–N4	164.52(7)

Continued on next page.

Continued.

$[Cu_6(O_2CCH_3)_8(tmsaec)]\cdot 2CH_3CN\cdot 11H_2O$ (**7**$\cdot 2CH_3CN\cdot 11H_2O$)					
Cu1–O1	1.925(5)	Cu2–O1	1.973(4)	Cu3–O3	1.898(5)
Cu1–O5	1.996(5)	Cu2–O2	2.343(5)	Cu3–O11	2.429(9)
Cu1–O7	2.194(4)	Cu2–O6	1.945(5)	Cu3–O12	2.008(7)
Cu1–N1	2.059(6)	Cu2–O8	1.936(5)	Cu3–N2	2.097(6)
Cu1–N3	1.936(5)	Cu2–O9	1.928(7)	Cu3–N4	1.930(7)
Cu1–O1–Cu2	105.1(2)				
O1–Cu1–O5	89.6(2)	O1–Cu2–O2	73.1(2)	O3–Cu3–N2	166.9(2)
O1–Cu1–O7	89.3(2)	O1–Cu2–O6	88.4(2)	O3–Cu3–N4	93.9(3)
O5–Cu1–O7	101.9(2)	O1–Cu2–O8	92.5(2)	N2–Cu3–N4	84.3(3)
O1–Cu1–N1	176.9(2)	O1–Cu2–O9	159.7(3)		
O1–Cu1–N3	91.5(2)	O2–Cu2–O6	101.7(2)		
N1–Cu1–O5	92.2(2)	O2–Cu2–O8	97.8(2)		
N1–Cu1–O7	92.8(2)	O2–Cu2–O9	86.8(3)		
N1–Cu1–N3	85.5(2)	O6–Cu2–O8	159.8(2)		
N3–Cu1–O5	142.6(2)	O6–Cu2–O9	93.1(2)		
N3–Cu1–O7	115.5(2)	O8–Cu2–O9	93.0(2)		

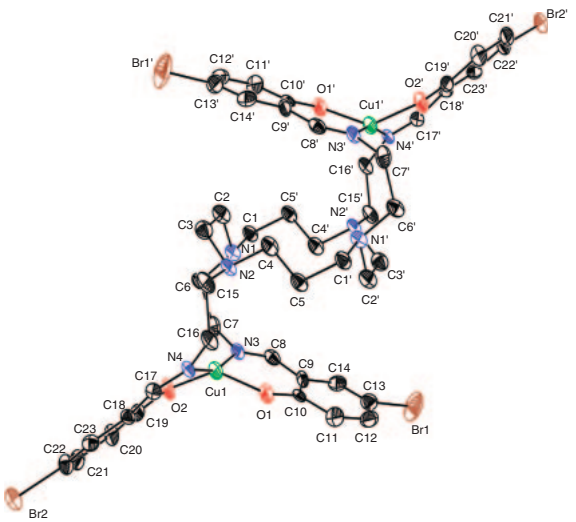

Figure 2. ORTEP drawing of the structure of $[Cu_2(tbsaec)]\cdot CHCl_3$ (**2**$\cdot CHCl_3$) showing the 50% probability thermal ellipsoids and atom numbering scheme. Hydrogen atoms and solvent molecules are omitted for clarity.

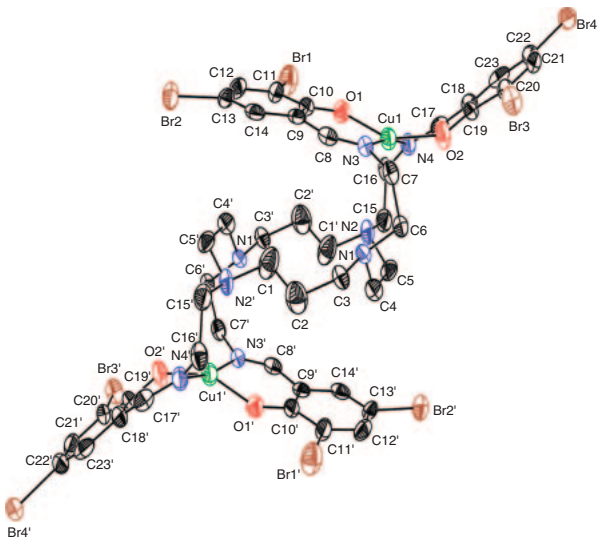

Figure 3. ORTEP drawing of the structure of $[Cu_2(tdbsaec)]\cdot 2/3CHCl_3\cdot 8/3H_2O$ (**3**$\cdot 2/3CHCl_3\cdot 8/3H_2O$) showing the 30% probability thermal ellipsoids and atom numbering scheme. Hydrogen atoms and solvent molecules are omitted for clarity.

ORTEP drawings of the molecular structures of **2**$\cdot CHCl_3$ and **3**$\cdot 2/3CHCl_3\cdot 8/3H_2O$, views of the molecular packing in the crystals of **4**$\cdot CHCl_3$ and **5**$\cdot 2/3CHCl_3\cdot 8/3H_2O$, and ORTEP drawing of the molecular structure of **6**$\cdot 2CH_3CN$ are shown in Figures 2, 3, 4, 5, and 6, respectively. The molecular structures of these complexes are similar to that of **1**$\cdot 2CHCl_3$, namely, the coordination geometry around the copper atom is a distorted square plane with two phenolic-oxygen atoms and two imino-nitrogen atoms of the two Schiff-base pendant arms. Considering the mean plane determined by the basal N_2O_2 atoms (with maximum deviations of ±0.45, ±0.32, ±0.47, ±0.32, and ±0.37 Å for **2**$\cdot CHCl_3$, **3**$\cdot 2/3CHCl_3\cdot 8/3H_2O$, **4**$\cdot CHCl_3$, **5**$\cdot 2/3CHCl_3\cdot 8/3H_2O$, and **6**$\cdot 2CH_3CN$, respectively), the Cu atom is displaced only slightly (less than 0.15 Å) from this plane. The Cu–O and Cu–N distances are 1.887(5)–1.956(5) and 1.936(2)–1.975(6) Å, respectively. The intramolecular Cu···Cu′ distances are 8.692(2) and 8.949(2) Å for **2**$\cdot CHCl_3$, 8.789(7) Å for **3**$\cdot 2/3CHCl_3\cdot 8/3H_2O$, 8.734(1) and 8.905(2) Å for **4**$\cdot CHCl_3$, 8.752(3) Å for **5**$\cdot 2/3CHCl_3\cdot 8/3H_2O$, and 8.813(2) Å for **6**$\cdot 2CH_3CN$, respectively. It is noteworthy that the crystal packing modes are totally different between the monosubstituted and disubstituted derivatives as shown in Figures 4 and 5. In the formers (**2**$\cdot CHCl_3$ and **4**$\cdot CHCl_3$), the crystals contain chloroform molecules, forming closer intermolecular contact with the aromatic carbon atoms of the Schiff-base ligands. On the other hand, in the latter crystals (**3**$\cdot 2/3CHCl_3\cdot 8/3H_2O$ and **5**$\cdot 2/3CHCl_3\cdot 8/3H_2O$), a small cavity is formed by the crystallographic symmetry of the trigonal system, where chloroform as well as water molecules are housed. In the crystal of **6**$\cdot 2CH_3CN$, the closest intermolecular contact exists between the carbon atoms of the naphthyl groups

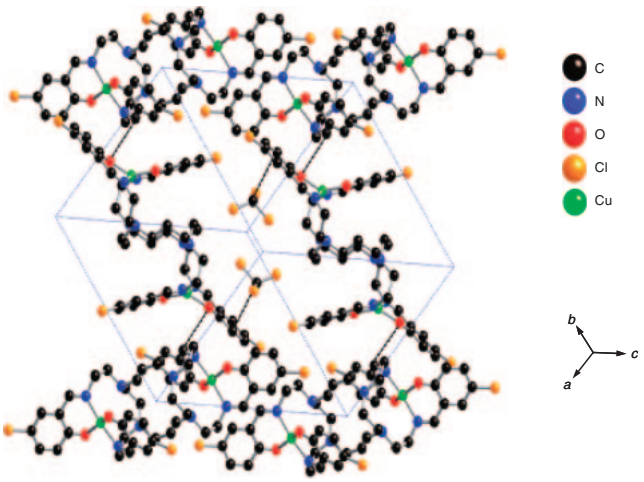

Figure 4. Crystal packing diagram of $[Cu_2(tcsaec)]\cdot CHCl_3$ (**4**$\cdot CHCl_3$). Hydrogen atoms are omitted for clarity.

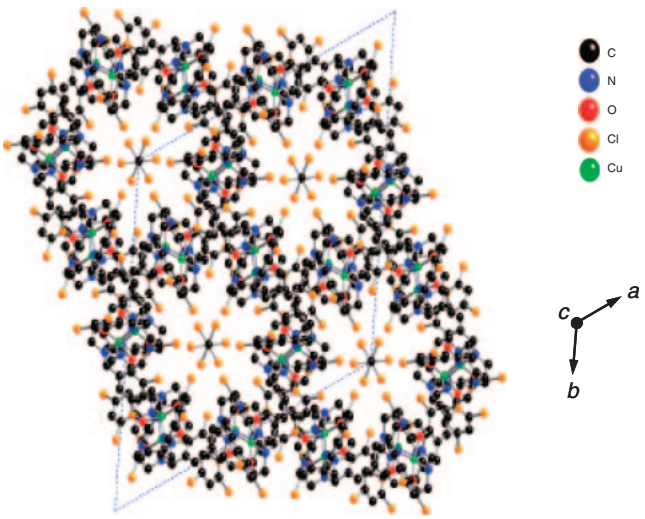

Figure 5. Crystal packing diagram of $[Cu_2(tdcsaec)]\cdot 2/3CHCl_3\cdot 8/3H_2O$ (**5**$\cdot 2/3CHCl_3\cdot 8/3H_2O$). Hydrogen atoms and water molecules are omitted for clarity.

with the C16···C22 ($1-x$, $y+1/2$, $1/2-z$) distance being 3.559(3) Å in the face to edge mode.

Hexanuclear Copper(II) Complex with Acetate as the Additional Ligands, $[Cu_6(O_2CCH_3)_8(tmsaec)]$. When copper(II) acetate was treated with the Schiff-base ligand, H_4tmsaec, by a template reaction a hexanuclear copper(II) complex with acetate, $[Cu_6(O_2CCH_3)_8(tmsaec)]\cdot 3H_2O$ (**7**$\cdot 3H_2O$), was isolated as dark green crystals. Single crystals suitable for X-ray diffraction study were obtained as $[Cu_6(O_2CCH_3)_8(tmsaec)]\cdot 2CH_3CN\cdot 11H_2O$ (**7**$\cdot 2CH_3CN\cdot 11H_2O$). The crystal structure of this complex was determined by X-ray crystal structure analysis. The ORTEP drawing of the molecular structure of **7**$\cdot 2CH_3CN\cdot 11H_2O$ is shown in Figure 7. The molecule has a crystallographic inversion center at the center of the macrocyclic ring. In the asymmetric unit, a half of the hexanuclear molecule, two copper atoms (Cu1 and Cu2) are bound by one Schiff-base pendant arm with two bridging acetate ions and one copper atom (Cu3) is coordinated by another Schiff-base pendant arm with one acetate ion. The

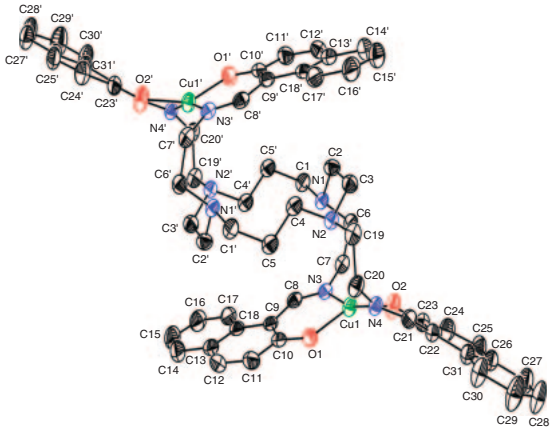

Figure 6. ORTEP drawing of the structure of $[Cu_2(tnaec)]\cdot 2CH_3CN$ (**6**$\cdot 2CH_3CN$) showing the 35% probability thermal ellipsoids and atom numbering scheme. Hydrogen atoms and solvent molecules are omitted for clarity.

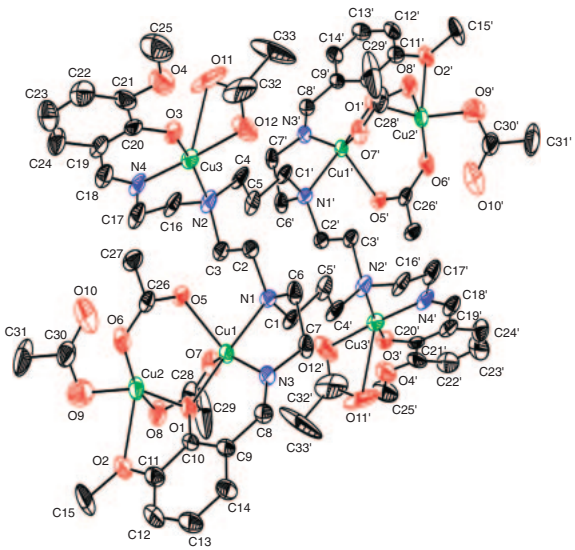

Figure 7. ORTEP drawing of the structure of $[Cu_6(O_2CCH_3)_8(tmsaec)]\cdot 2CH_3CN\cdot 11H_2O$ (**7**$\cdot 2CH_3CN\cdot 11H_2O$) showing the 35% probability thermal ellipsoids and atom numbering scheme. Hydrogen atoms and solvent molecules are omitted for clarity.

three copper(II) sites are different. The coordination geometry around the Cu1 is trigonal bipyramidal, with the copper atom being surrounded by the imino-nitrogen atom (N3) of the Schiff-base arm [Cu1–N3 1.936(5) Å], two oxygen atoms of the bridging acetato groups (O5 and O7) [Cu1–O5 1.996(5) Å, Cu1–O7 2.194(4) Å] in the equatorial positions. The axial positions of the trigonal bipyramid are occupied by the bridging phenoxo-oxygen atom (O1) and the amino-nitrogen atom (N1) of the macrocyclic ring moiety with an O1–Cu1–N1 angle of 176.9(2)°. The angles around the copper(II) atom in the basal plane vary from 101.9(2) to 142.6(2)°, indicating a distorted trigonal bipyramidal geometry. Such a distortion can be quantitatively characterized using the parameter τ as defined by Addison et al. ($\tau = 1$ for a regular trigonal bipyramid and 0 for a square-based pyramid).[11] The calculated value $\tau = 0.57$ indicates that the polyhedron around the Cu1 atom is closer to a

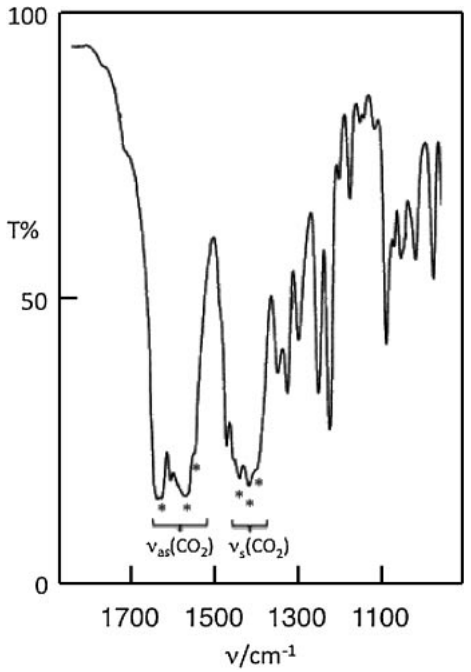

Figure 8. Infrared spectra of $[Cu_6(O_2CCH_3)_8(tmsaec)]$ (**7**). The asterisks indicate the $\nu_{as}(CO_2)$ and $\nu_s(CO_2)$ bands.

trigonal-bipyramidal geometry. The coordination sphere around Cu2 atom is square pyramidal with $\tau = 0.002$, consisting of the bridging phenoxo-oxygen atom (O1) of the Schiff-base arm (Cu2–O1 1.973(4) Å) and two bridging acetato-oxygen atoms (O6 and O8) [Cu2–O6 1.945(5) Å, Cu2–O8 1.936(5) Å], a monodentate acetato-oxygen atom (O9) [Cu2–O9 1.928(7) Å], in the equatorial plane and the methoxy-oxygen atom of the Schiff-base arm (O2) [Cu2–O2 2.343(5) Å] in the apical position. The Cu3 coordination sphere is rather irregular; it can be described as a distorted square pyramid with the long axial contact to the oxygen atom (O11) of the acetato group [Cu3–O11 2.429(9) Å]. The three copper atoms are located at the corners of a distorted isosceles triangle with Cu1–Cu2 3.096(1) Å, Cu1–Cu3 5.302(1) Å, and Cu2–Cu3 6.286(2) Å. It is noteworthy that three kinds of coordination modes of acetate ions can be found in the same molecule: monodentate, bidentate, and bridging. This is in harmony with the observed $\nu_{as}(CO_2)$ and $\nu_s(CO_2)$ bands in the IR spectrum. In the IR spectra of the complex, three strong bands of the vibrations of carboxylato groups can be found at 1620, 1569, and 1540 cm^{-1} which can be attributable to antisymmetric $\nu_{as}(CO_2^-)$ stretching bands and another three strong peaks appear at 1439, 1416, and 1390 cm^{-1} which can be assigned to symmetric $\nu_s(CO_2^-)$ stretching bands (Figure 8). The Δ values of $\nu_{as}(CO_2^-) - \nu_s(CO_2^-)$, $1620 - 1390 = 230\,cm^{-1}$, $1569 - 1416 = 153\,cm^{-1}$, and $1540 - 1439 = 101\,cm^{-1}$, are in the ranges of those of the monodentate-, bridging-, and bidentate-acetato complexes, repectively.[12] Although there are many types of coordination modes of acetate ion in the literatures,[13] this is a novel example which one molecule has different types of coordination to a metal center.[14] Another interesting point of this complex is the two different coordination geometries of the phenoxo-bridged dinuclear moiety: the trigonal-bipyramidal copper (Cu1) and the square-pyramidal copper (Cu2) are triply

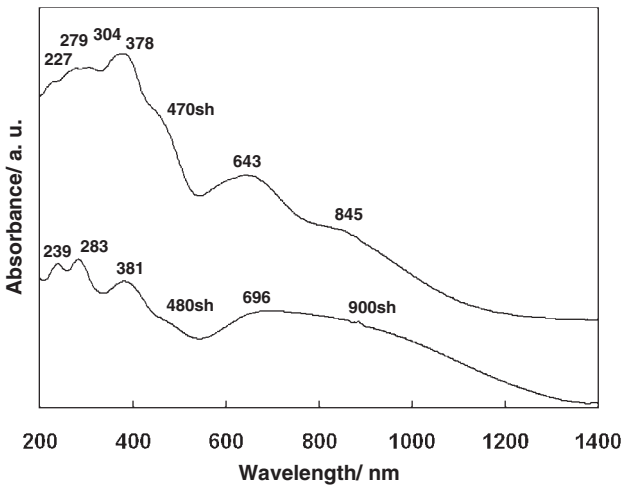

Figure 9. Diffuse reflectance spectra of $[Cu_2(tsaec)]$ (**1**) (upper) and $[Cu_6(O_2CCH_3)_8(tmsaec)]$ (**7**) (lower).

bridged by the phenoxo-oxygen and two *syn–syn* acetato groups. The cyclam ring moiety takes the trans III form contrary to the cases of **1**–**6**, dinuclear manganese(III) complexes of this type of Schiff-base ligands,[5] and dinuclear palladium(II) complex with the tosylated ligand, $(tstaec^{4-})$,[4] in which the macrocyclic ring takes the trans IV form. The trans III form can be found in dinuclear metal complexes with taec.[3] In these complexes, the nitrogen atoms of the cyclam ring moiety participate in coordination to metal centers. In **7**, all of the cyclam nitrogen atoms do coordinate to the Cu atoms. As a whole, the $tmsaec^{4-}$ ligand binds six copper atoms by the use of four Schiff-base pendant arms below and above the cyclam ring moiety. In the crystal, the closest intermolecular Cu···Cu separation is 6.472(2) Å between Cu1···Cu2 $(x + 1/2, -y - 1/2, z + 1/2)$.

Electronic Spectra of Complexes 1–7. The UV–visible spectra of the present complexes were measured by diffuse reflectance spectra, because most of them are insoluble in water and organic solvents. The diffuse reflectance spectra of **1** and **7** are shown in Figure 9 as representative examples. The complexes show three strong bands (226–239, 279–315, and 341–401 nm) in the UV region, a shoulder at 470 nm, and a broad band at 642–660 nm with shoulder at 790–845 nm in the visible region. The intense UV region bands can be assigned to the transitions of the ligand itself including a π–π^* transition of imino (RHC=N–) group in origin, because the Schiff-base ligands have similar bands in the UV region.[15] The intense 341–401 nm band or the shoulder around 470 nm may be assigned by analogy to other copper(II) complexes as a LMCT band from the phenoxo-oxygen to the Cu^{II} d orbital.[16] The visible region bands of **1**–**6** are almost identical and can be associated with d–d transitions, confirming the similar coordination environments of the copper(II) atoms. This spectral feature is consistent with square-planar copper(II) ion surrounded by N_2O_2 donor atoms.[17] In the case of the hexanuclear complex, **7**, the diffuse reflectance spectra shows six bands at 239, 283, 381, 480sh, 696, and 900sh nm. Compared with those of the dinuclear complexes, the d–d bands are broader and shifted to a little lower frequency region reflecting the coexistence of square-pyramidal and trigonal-bipyramidal

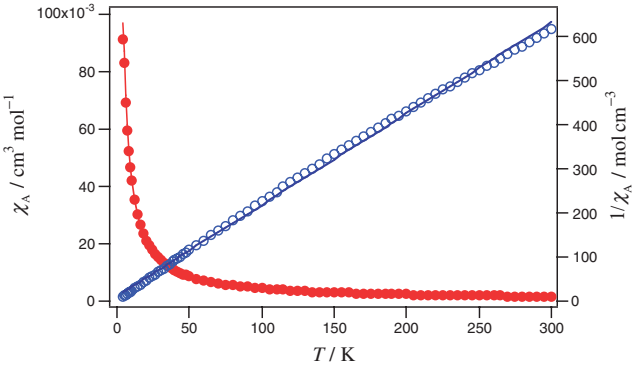

Figure 10. Temperature dependence of magnetic susceptibility (●) and inverse magnetic susceptibility (○) of [Cu_2(tnaec)] (**6**). Solid line for magnetic susceptibility was drawn with the parameters $g = 2.1$ (fixed), $J = 0.4\,cm^{-1}$ for eq 1.

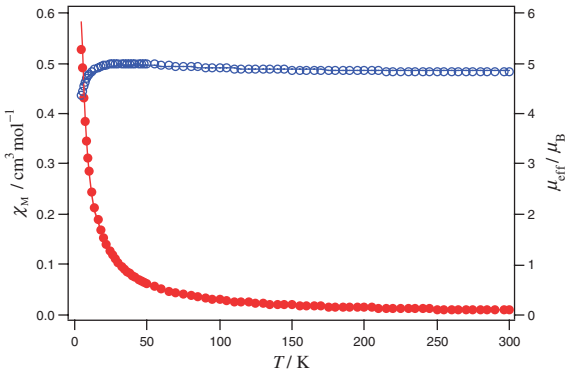

Figure 11. Temperature dependence of magnetic susceptibility (●) and magnetic moment (○) of [$Cu_6(O_2CCH_3)_8$(tmsaec)] (**7**). Solid lines were drawn with the parameters $g_1 = 2.16$, $J = -1.7\,cm^{-1}$, $g_2 = 2.21$, and $\theta = 0.49\,K$ for eq 2.

geometries.[17] In DMSO solution, the complex shows two absorptions at 384 and 670 nm with molar extinction coefficients of 2630 and 132 $M^{-1}\,cm^{-1}$/Cu, respectively, showing the latter band should be d–d transitions.

Magnetic Properties of Complexes 1–7. The temperature dependence of the magnetic susceptibilities of **1**–**7** was measured on powdered samples in the temperature range of 4.5–300 K. The magnetic data of **6** are shown in Figure 10 in the form of χ_A and $1/\chi_A$ vs. T plots as a representative example. The temperature dependence of magnetic data show Curie–Weiss behavior, $\chi_A = C/(T-\theta)$, with a Weiss constant ($\theta = -1.5$ K for **1**, -1.4 K for **2**, -3.9 K for **3**, -0.7 K for **4**, -2.5 K for **5**, and -5.5 K for **6**), suggesting a weak antiferromagnetic interaction between the copper(II) ions for the complexes. The magnetic moments of **1**–**6** at 300 K are in the range of 1.73–1.97 μ_B (per Cu^{II} unit), which is close to the spin-only value (1.73 μ_B) of Cu^{II} ($S = 1/2$) ion. The magnetic moments remain essentially constant upon lowering the temperature to 4.5 K [the magnetic moments at 4.5 K are 1.69–1.81 μ_B (per Cu^{II} unit) for **1**–**6**], suggesting almost no magnetic interaction between copper(II) ions. Taking account of the dinuclear structures for these complexes, the magnetic data were analyzed with the Bleaney–Bowers equation based on the Heisenberg model ($H = -2JS_1 \cdot S_2$ ($S_1 = S_2 = 1/2$)):[18]

$$\chi_A = [Ng^2{\mu_B}^2/kT][3 + \exp(-2J/kT)]^{-1} + N\alpha \qquad (1)$$

where J is an exchange integral for the two copper(II) ions and the other symbols have their usual meanings.

The best-fitting parameters were obtained by fixing g and $N\alpha$ at 2.1 and $60 \times 10^{-6}\,cm^3\,mol^{-1}$, respectively: $J = -1.4\,cm^{-1}$ for **1**, $J = -0.8\,cm^{-1}$ for **2**, $J = -1.2\,cm^{-1}$ for **3**, $J = -0.7\,cm^{-1}$ for **4**, $J = -0.9\,cm^{-1}$ for **5**, and $J = 0.4\,cm^{-1}$ for **6**. The obtained J values are very small, showing that the magnetic interaction between the two copper(II) ions can be negligibly weak. This can be understandable, because the two copper(II) ions are well separated by the saturated macrocyclic ring with the long Cu···Cu distance, having no pathway to interact with each other.

The magnetic data of **7** are shown in Figure 11. At 300 K, the magnetic moment of **7** is 4.84 μ_B (per Cu^{II}_6 unit), being higher than the spin-only value (4.24 μ_B) which is expected for six noninteracting copper(II) ions for **7**. The magnetic moment slightly increases as the temperature is decreased from 300 to 40 K to reach the maximum value of 5.00 μ_B. Below 40 K, the magnetic moment decreases to reach a value of 4.35 μ_B at 4.5 K. The decrease in the magnetic moment could be mainly regarded as the contribution of antiferromagnetic interactions between copper(II) centers. The magnetic data of **7** were analyzed with the magnetic susceptibility equation based on a model consisting of two dinuclear copper(II) centers and two mononuclear copper(II) centers estimating the interaction between the dinuclear unit and mononuclear unit by introducing the Weiss constant, θ:

$$\chi_M = (4N{g_1}^2{\mu_B}^2/kT)[3 + \exp(-2J/kT)]^{-1} + N{g_2}^2{\mu_B}^2/[2k(T-\theta)] + 6N\alpha \qquad (2)$$

where J is the exchange integral for the two closest copper(II) atoms, θ is the Weiss temperature to account for the weak interaction between the mononuclear and dinuclear units and/or the intermolecular interaction, and the other symbols have the usual meanings. The best fitting parameters were obtained by fixing $N\alpha$ at $60 \times 10^{-6}\,cm^3\,mol^{-1}$. The obtained values are $g_1 = 2.16$, $J = -1.7\,cm^{-1}$, $g_2 = 2.21$, and $\theta = 0.49$ K. If we assume $g_1 = g_2 = 2.1$ in eq 2, we obtain the parameters $J = 32\,cm^{-1}$ and $\theta = -7.7$ K. The latter parameters show that a ferromagnetic interaction is operating between the closest copper atoms. However, the J value is too large as the coupling within the μ-phenoxo-di-μ-acetato dinuclear unit and the $-\theta$ value is also too large for the long Cu···Cu separations except the Cu1···Cu2. Therefore the former parameters are more realistic. Thus we can consider that weak antiferromagnetic interaction is operating between the closest two copper(II) atoms with the μ-phenoxo-di-μ-acetato bridges. A small θ value suggests that the interaction between the mononuclear and dinuclear units and/or the intermolecular interactions are very weak. In **7**, the Cu1 atom has a distorted trigonal-bipyramidal environment and the Cu2 atom is in a square-pyramidal geometry and thus magnetic orbitals of the Cu1 and Cu2 atoms will be mainly d_{z^2} and $d_{x^2-y^2}$, respectively.[19] The bridging phenoxo-oxygen O1 atom is in an apical position for

the Cu1 atom and equatorial position to the Cu2 atom. Thus, it has bonding interactions with the d_{z^2} and $d_{x^2-y^2}$ orbitals of the Cu1 and Cu2 atoms, respectively. The Cu1–O1–Cu2 angle is 105.2(2)°, which is preferable for antiferromagnetic interaction,[20–22] although the interaction is weak. For the two acetato bridges, the magnetic orbital is oriented along the equatorial direction of the square pyramid of the Cu2 atom toward the bridging acetato orbitals and the other carboxylato-oxygen orbitals are bonded to the equatorial sites of the trigonal-bipyramidal Cu1 which have no magnetic orbital. Thus, the unpaired electron of the Cu2 atom does not seem to be able to interact with that of the Cu1 atom through the acetato bridges. However, the distortion to the square-pyramidal geometry of the Cu1 atom may lessen the antiferromagnetic contribution to exchange through the phenoxo-bridge and allow the interaction through the bridging acetato groups, resulting in an overall weak interaction.

Conclusion

The Schiff-base ligands based on the cyclam, 1,4,8,11-tetrakis(salicylideneaminoethyl)-1,4,8,11-tetraazacyclotetradecane (H_4tsaec) and its substituent derivatives, bind two copper(II) ions with the four Schiff-base pendant arms outside the cyclam ring, giving a series of dinuclear copper(II) complexes with a long Cu···Cu distance of 8.692(2)–8.949(2) Å. On the other hand, the methoxy-substituent derivative, 1,4,8,11-tetrakis(3-methoxysalicylideneaminoethyl)-1,4,8,11-tetraazacyclotetradecane, binds six copper(II) ions with the four pendant arms by virtue of the donor property of the methoxy-oxygen atoms, giving a novel system containing three kinds of coordination modes of acetate ions (monodentate, bidentate, and bridging) in the same molecule. This is in contrast with the cases for the manganese systems,[5] reflecting the combination of the present cyclam-based Schiff-base ligands and metal ions.

This present work was partially supported by Grants-in-Aid for Scientific Research No. 19550074 from the Ministry of Education, Culture, Sports, Science and Technology.

References

1 a) P. V. Bernhardt, G. A. Lawrance, *Coord. Chem. Rev.* **1990**, *104*, 297. b) V. Alexander, *Chem. Rev.* **1995**, *95*, 273. c) K. P. Wainwright, *Coord. Chem. Rev.* **1997**, *166*, 35. d) S. F. Lincoln, *Coord. Chem. Rev.* **1997**, *166*, 255. e) M. Meyer, V. Dahanoui-Gindrey, C. Lecomte, R. Guilard, *Coord. Chem. Rev.* **1998**, *178–180*, 1313. f) K. P. Wainwright, *Adv. Inorg. Chem.* **2001**, *52*, 293. g) I. Lukes, J. Kotek, P. Vojtisek, P. Hermann, *Coord. Chem. Rev.* **2001**, *216–217*, 287.

2 a) D. Parker, *Chem. Soc. Rev.* **1990**, *19*, 271. b) S. Jurisson, D. Berning, W. Jia, D. Ma, *Chem. Rev.* **1993**, *93*, 1137. c) P. Caravan, J. J. Ellison, T. J. McMurry, R. B. Lauffer, *Chem. Rev.* **1999**, *99*, 2293. d) D. Parker, R. S. Dickins, H. Puschmann, C. Crossland, J. A. K. Howard, *Chem. Rev.* **2002**, *102*, 1977. e) S. Zhang, M. Merritt, D. E. Woessner, R. E. Lenkinski, A. D. Sherry, *Acc. Chem. Res.* **2003**, *36*, 783. f) S. Liu, *Chem. Soc. Rev.* **2004**, *33*, 445. g) E. Toth, L. Helm, A. E. Merbach, in *Comprehensive Coordination Chemistry II*, ed. by J. A. McCleverty, T. J. Meyer, Elsevier, Amsterdam, **2004**, Vol. 9, pp. 841–881.

3 a) I. Murase, M. Mikuriya, H. Sonoda, S. Kida, *J. Chem. Soc., Chem. Commun.* **1984**, 692. b) I. Murase, M. Mikuriya, H. Sonoda, Y. Fukuda, S. Kida, *J. Chem. Soc., Dalton Trans.* **1986**, 953. c) S. Kida, I. Murase, C. Harada, L. Daizeng, M. Mikuriya, *Bull. Chem. Soc. Jpn.* **1986**, *59*, 2595. d) M. Mikuriya, S. Kida, I. Murase, *J. Chem. Soc., Dalton Trans.* **1987**, 1261. e) M. Mikuriya, S. Kida, I. Murase, *Bull. Chem. Soc. Jpn.* **1987**, *60*, 1355. f) M. Mikuriya, S. Kida, I. Murase, *Bull. Chem. Soc. Jpn.* **1987**, *60*, 1681. g) M. Mikuriya, S. Kida, T. Kohzuma, I. Murase, *Bull. Chem. Soc. Jpn.* **1988**, *61*, 2666. h) M. Mikuriya, I. Murase, E. Asato, S. Kida, *Chem. Lett.* **1989**, 497. i) A. Evers, R. D. Hancock, I. Murase, *Inorg. Chem.* **1986**, *25*, 2160. j) E. Asato, S. Kida, I. Murase, *Inorg. Chem.* **1989**, *28*, 800. k) G. Vuckovic, E. Asato, N. Matsumoto, S. Kida, *Inorg. Chim. Acta* **1990**, *171*, 45. l) H. Harada, M. Kodera, G. Vuckovic, N. Matsumoto, S. Kida, *Inorg. Chem.* **1991**, *30*, 1190. m) L. H. Tan, M. R. Taylor, K. P. Wainwright, P. A. Duckworth, *J. Chem. Soc., Dalton Trans.* **1993**, 2921. n) R. Newell, A. Appel, D. L. DuBois, M. R. DuBois, *Inorg. Chem.* **2005**, *44*, 365. o) A. M. Appel, R. Newell, D. L. DuBois, M. R. DuBois, *Inorg. Chem.* **2005**, *44*, 3046.

4 S. Wada, T. Kotera, M. Mikuriya, *Bull. Chem. Soc. Jpn.* **2008**, *81*, 1454.

5 a) M. Mikuriya, Y. Yamazaki, *Chem. Lett.* **1995**, 373. b) S. Wada, M. Mikuriya, in *Achievement in Coordination, Bioinorganic and Applied Inorganic Chemistry*, ed. by M. Melnik, J. Sima, M. Tatarko, Slovak Technical University Press, Bratislava, **2007**, pp. 201–207. c) S. Wada, M. Mikuriya, *Bull. Chem. Soc. Jpn.* **2008**, *81*, 348.

6 a) M. Mikuriya, H. Takebayashi, K. Matsunami, *Bull. Chem. Soc. Jpn.* **1994**, *67*, 3128. b) M. Mikuriya, K. Matsunami, *Mater. Sci.-Pol.* **2005**, *23*, 773. c) M. Mikuriya, R. Nukada, W. Tokii, Y. Hashimoto, T. Fujii, *Bull. Chem. Soc. Jpn.* **1996**, *69*, 1573. d) M. Mikuriya, T. Fujii, T. Tokii, A. Kawamori, *Bull. Chem. Soc. Jpn.* **1993**, *66*, 1675. e) M. Mikuriya, K. Majima, Y. Yamato, *Chem. Lett.* **1992**, 1929. f) M. Mikuriya, Y. Yamato, T. Tokii, *Chem. Lett.* **1992**, 1571. g) M. Mikuriya, Y. Yamato, T. Tokii, *Bull. Chem. Soc. Jpn.* **1992**, *65*, 1466. h) M. Mikuriya, Y. Yamato, T. Tokii, *Bull. Chem. Soc. Jpn.* **1992**, *65*, 2624. i) M. Mikuriya, K. Nakadera, T. Kotera, T. Tokii, W. Mori, *Bull. Chem. Soc. Jpn.* **1995**, *68*, 3077. j) M. Mikuriya, Y. Hashimoto, A. Kawamori, *Chem. Lett.* **1995**, 1095. k) M. S. Shongwe, M. Mikuriya, R. Nukada, E. W. Ainscough, A. M. Brodie, J. M. Waters, *Inorg. Chim. Acta* **1999**, *290*, 228. l) C. Palopoli, B. Chansou, J.-P. Tuchagues, S. Signorella, *Inorg. Chem.* **2000**, *39*, 1458.

7 *Molecular Magnetism*, ed. by O. Kahn, VCH Publishers, New York, **1993**, p. 3.

8 *SHELXTL-NT, v. 5.10*, Bruker AXS, Inc., Madison, WI, **1999**.

9 a) M. Mikuriya, T. Izumitani, H. Okawa, S. Kida, *Bull. Chem. Soc. Jpn.* **1986**, *59*, 2941. b) M. Calligaris, G. Nardin, L. Randaccio, *Coord. Chem. Rev.* **1972**, *7*, 385.

10 B. Bosnich, C. K. Poon, M. L. Tobe, *Inorg. Chem.* **1965**, *4*, 1102.

11 A. W. Addison, T. N. Rao, J. Reedijk, J. van Rijn, G. C. Verschoor, *J. Chem. Soc., Dalton Trans.* **1984**, 1349.

12 *Infrared and Raman Spectra of Inorganic and Coordination Compounds, Part B*, 6th ed., ed. by K. Nakamoto, John and Wiley & Sons, Inc., Hoboken, **2009**, p. 64.

13 M. Mikuriya, *Bull. Jpn. Soc. Coord. Chem.* **2008**, *52*, 17.

14 R. Horikoshi, M. Mikuriya, *Bull. Chem. Soc. Jpn.* **2005**, *78*, 827.

15 C. R. K. Rao, P. S. Zacharias, *Polyhedron* **1997**, *16*, 1201.

16 a) R. C. Holz, J. M. Brink, F. T. Gobena, C. J. O'Connor, *Inorg. Chem.* **1994**, *33*, 6086. b) T. N. Sorrell, C. J. O'Connor, O. P. Anderson, J. H. Reibenspies, *J. Am. Chem. Soc.* **1985**, *107*, 4199. c) L. Cai, W. Xie, H. Mahmoud, Y. Han, D. J. Wink, S. Li, C. J. O'Connor, *Inorg. Chim. Acta* **1997**, *263*, 231.

17 Y. Murakami, K. Sakata, in *Kireto-Kagaku*, ed. by K. Ueno, Nankodo, Tokyo **1976**, Vol. 1, pp. 211–221.

18 B. Bleaney, K. D. Bowers, *Proc. R. Soc. A* **1952**, *214*, 451.

19 S. Laborda, R. Clérac, C. E. Anson, A. K. Powell, *Inorg. Chem.* **2004**, *43*, 5931.

20 L. K. Thompson, S. K. Mandal, S. S. Tandon, J. N. Bridson, M. K. Park, *Inorg. Chem.* **1996**, *35*, 3117.

21 J. Lorösch, U. Quotschalla, W. Haase, *Inorg. Chim. Acta* **1987**, *131*, 229.

22 C. R. Choudhury, S. K. Dey, R. Karmakar, C.-D. Wu, C.-Z. Lu, M. S. E. Fallah, S. Mitra, *New J. Chem.* **2003**, *27*, 1360.